J|A|C|S
COMMUNICATIONS

Published on Web 04/07/2007

X-Shaped Rigid Arylethynes to Mediate the Assembly of Nanoparticles

I-Im S. Lim,† Christopher Vaiana,† Zhi-Yang Zhang,‡ Ying-Jun Zhang,‡ De-Lie An,*,‡ and Chuan-Jian Zhong*,†

Department of Chemistry, State University of New York at Binghamton, Binghamton, New York 13902, and Department of Chemistry, College of Chemistry and Chemical Engineering, Hunan University, Changsha, Hunan, 410082, China

Received February 22, 2007; E-mail: cjzhong@binghamton.edu; deliean@sina.com

The ability to control interparticle spatial properties of nanoparticle assemblies is one of the major challenges for the design and understanding of functional nanostructures. Molecular linkers or mediators, including DNAs,[1] amino acids,[2] polymers or surfactants,[3−4] dyes,[5] and multidentate thioethers[6] have been exploited for such control. The control has also involved various assembly processes such as place-exchange reaction,[7] layer-by-layer stepwise assembly,[8] exchange-crosslinking,[9] and mediator-template assembly.[6] Potential applications of the nanoparticle assemblies include chemical sensors or biosensors, biomedical diagnostics, information storage, and catalysis.[10−11] Despite these advances, our fundamental understanding on controlling interparticle spatial properties remains very limited. On the basis of the demonstration of mediator-template assembly using methylthio silanes as mediators,[6] one intriguing question is how the interparticle spatial properties of nanoparticle assemblies can be tuned by size, shape, and binding properties of the mediators. The answer would have a profound impact on the fine-tunability of the assembled nanostructures, which requires novel designs of the mediator structures in terms of size, shape, and ligand properties. Recent advances in the synthesis of methylthio functionalized structures with different sizes and shapes[12] create an opportunity for such design. We demonstrate herein the assembly of molecularly capped gold nanoparticles by X-shaped methylthio arylethynes (MTA) which are tailorable in size and binding properties (Scheme 1). The X−MTAs consist of a central benzene ring with four symmetrically attached methylthio legs featuring structural rigidity, π-conjugation, and shape/size tunability. The subtle difference in the structure next to the methylthio group, e.g., with (X) or without (X′) a triple bond, provides fine-tuning of its coordinating properties to gold.

A model calculation of the partial charge (δ_+) on S groups reveals +0.61e and +0.46e for X- and X′-MTAs, respectively (see Supporting Information (SI)). In addition to the control of interparticle spatial properties, these structural attributes may lead to unique optical and spectroscopic properties. For example, the interparticle interaction plays an important role ("hot spots") in surface-enhanced Raman scattering (SERS).[13] How the electronic or structural effects are operative in the interparticle spatial properties constitutes an intriguing question for exploring the fundamental basis of the SERS effect.

The synthesis of gold nanoparticles capped with a tetraoctylammonium (TOA^+) bromide shell (Au@TOA with a Au core diameter of 5∼6 nm)[6] and the synthesis of X-MTA and X′-MTA are described in the SI. The reactivities for X- and X′-MTA mediated assembly of Au@TOA were examined by monitoring the spectral evolution of the surface plasmon (SP) resonance band. Figure 1A shows a representative set of spectral evolution for the assembly

Scheme 1. X-Shaped Arylethynes with (X (A)) and without (X′ (B)) a Triple Bond Next to Each of the Methylthio Groups

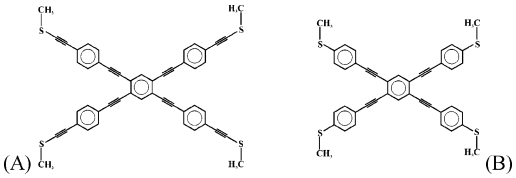

of Au@TOA mediated by X- (a) and X′-MTA (b) in a toluene solution. Upon addition of MTAs into the nanoparticle solution in a controlled concentration ratio, a decrease in the 520 nm band and an increase in the longer-wavelength band are evident. There is a distinct difference in the characteristics of spectral evolution between X- and X′-MTA assembly processes. The spectral evolution of X-MTA assembly (a) expands to a much longer wavelength region than that for X′-MTA (b) (Figure 1A inserts), suggesting that the extent of the assembly growth is larger for X- than for X′-MTA. The increase of assembly size as a function of time was confirmed by dynamic light scattering measurement with a similar system (see SI).

The assembly rate for X′-MTA (b) is found to be much faster than that for X-MTA (a) at the same concentration. The apparent rate constants (k, first-order) for X- and X′-MTA were 7.72×10^{-4} and 3.75×10^{-3} s^{-1}, respectively. Remarkably, the assembly rate difference is also reflected by the disassembly rate difference observed upon adding decanethiol (DT) into the solution (−SH is a stronger binding ligand to Au than −S− group). The disassembly displayed a much faster rate as shown by the decrease of the 700-nm band and the increase of the 530-nm band for X′-MTA assembly (Figure 1B). The apparent rate constants (first-order) for the disassembly of X− and X′-MTA assemblies were found to be 1.05×10^{-2} and 2.72×10^{-1} s^{-1} (530-nm band), and 6.09×10^{-3} and 1.70×10^{-1} s^{-1} (700-nm band), respectively, which reflects both structural and electronic differences between X- and X′-MTA.

Examination of the morphology revealed further details of the nanoparticle assemblies (Figure 2). X-MTA is found to favor the

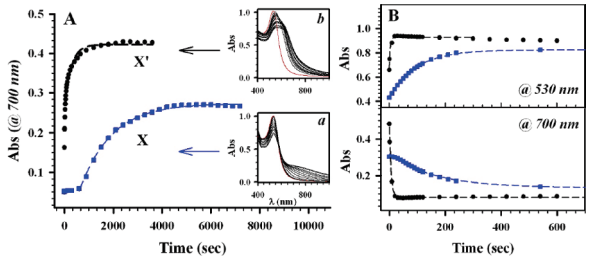

Figure 1. (A) Spectral evolution of SP band at 700 nm for the assembly of Au@TOA in toluene ([X]/[Au] = 17) by X- (a, ■) and X′- (b, ●) MTAs. The inserts show the SP band spectra. (B) Spectral evolution for DT-induced disassembly. ([DT] = 133 μM). The lines are based on first-order kinetics.

† State University of New York at Binghamton.
‡ Hunan University.

10.1021/ja071280m CCC: $37.00

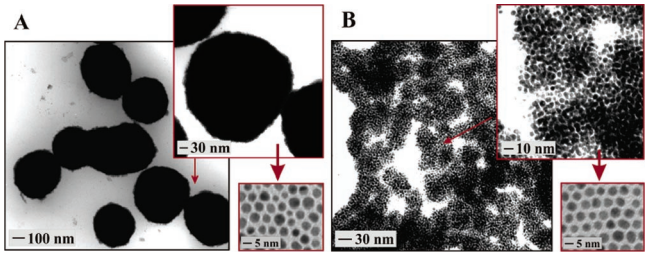

Figure 2. TEM micrographs for the mediated assembly of Au@TOA in toluene using X- (A) and X′-MTA (B) (Top inserts: magnified views) ([X]/[Au] =17). The bottom inserts show samples taken of the DT-induced disassembly of X- (A) and X′-MTA assembly (B). ([DT]/[X] = 83).

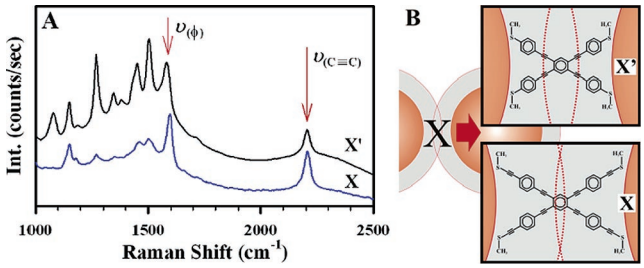

Figure 3. (A) SERS spectra for X- and X′-MTA mediated assemblies of Au@TOA. (B) Interparticle spacing for the two assemblies (scaled, see SI). The dotted lines illustrate relative penetration of the TOA shells.

growth of larger-sized assemblies than those for X′-MTA. Spherical assemblies with an average size of 350−400 nm are observed for X-MTA (A), in contrast to the average size of 40−60 nm for X′-MTA (B). The TEM images are representative of the characteristic sizes and shapes on the entire TEM grid for multiple samples, including those with lower magnifications. For samples taken after the DT-induced disassembly, ordered domains with a well-defined interparticle spacing are evident, in sharp contrast to the highly clustered features for the assembly (Figure 2 bottom inserts). The fact that these assemblies can be disassembled by addition of a thiol supports the reversibility of the assembly.

A close examination of the morphology of the assemblies in the TEM images suggests the presence of domains of packing order. Model calculations (see SI) indicate that the 4-leg symmetric interparticle linkage between two particles by X (or X′)-MTA seems to be the likely binding structure. A two-leg diagnostic interparticle linking is unlikely to be energetically favorable. The measured average edge-to-edge interparticle distance in Figure 2 showed ∼1.5 nm for X-MTA (see SI) and ∼1.3 nm for X′-MTA assembly. This subtle difference is consistent with the size difference between X and X′. For the disassembly, the comparable interparticle distances agree with DT-shell encapsulation in both cases.

The detection of SERS signatures characteristic of MTAs (Figure 3A) provides clear evidence for the adsorption of MTAs on gold nanoparticles. The peaks at 2206 and 1594 cm^{-1} arise from the triple bond ($\nu_{(C\equiv C)}$) and the benzene breathing ($\nu_{(\phi)}$) modes, respectively. The SERS effect was substantiated by control experiments, which showed no observable peaks for Au nanoparticles alone and MTA molecules alone under similar conditions. The relative intensity of these bands and the fine structures in 1000∼1600 cm^{-1} region reveal subtle differences between X and X′ assemblies, which likely reflects the interparticle structural and spacing differences (Figure 3B) in the "hot spots" responsible for the SERS effect.[13]

The interparticle binding strength and distance are defined by the structural and electronic properties of the MTA−TOA combination, which are responsible for the differences in the spectroscopic characteristics and the assembly size. On one hand, δ_+ (>S:) for X′-MTA is smaller than that for X-MTA (by 25%). On the other hand, the overall size of X′-MTA is smaller than X-MTA (by 20%). These differences explain the relative difference in the assembly rate. For X′-MTA, the smaller interparticle distance and the smaller δ_+ lead not only to a greater >S: → Au coordination bond strength but also a greater interpenetration of the TOA shells. TOA acts as both a capping and templating agent. The degree for the interparticle overlap of the TOA shells depends on the size of X (as shown by the gray regions outlined by dotted lines in Figure 3B). It is the compromised balance of these interactions that determines the assembly rate and size. Since it is an enthalpy-driven process,[6b] the extent for the interparticle shell penetration must have played a significant role in balancing the interactions. It is an experimental fact that the smaller extent of the intershell penetration favors the growth of larger-sized assemblies at a slower assembly rate. An increase in TOA^+ concentration (see SI) showed a reduced rate for X-MTA assembly and exhibited almost no effect on X′-MTA assembly, substantiating the important role of the intershell interaction in the assembly.

In conclusion, the assembly of gold nanoparticles mediated by X-shaped arylethynes has been demonstrated to form densely packed clusters in spherical shapes. The findings of the optical and spectroscopic properties of the assembly and disassembly tunable by two different sizes and partial charges of MTAs serve as the first demonstration of an interparticle structural tunability in terms of size, shape, and binding properties. Our ongoing work aims at the quantitative structural correlation and exploitation of the optical and SERS properties.

Acknowledgment. This work was supported by the NSF (Grant CHE0349040), and by the NNSFC (Grant No. 20272012). S.L. acknowledges support of the NSF Graduate Research Fellowship.

Supporting Information Available: Synthesis, modeling, and characterization. This material is available free of charge via the Internet at http://pubs.acs.org.

References

(1) Elghanian, R.; Storhoff, J. J.; Mucic, R. C.; Letsinger, R. L.; Mirkin, C. A. *Science* **1997**, *277*, 1078.
(2) Lim, I-I. S.; Ip, W.; Crew, E.; Njoki, P. N.; Mott, D.; Zhong, C. J. *Langmuir* **2007**, *23*, 826.
(3) (a) Frankamp, B. L.; Boal, A. K.; Rotello, V. M. *J. Am. Chem. Soc.* **2002**, *124*, 15146. (b) Zubarev, E. R.; Xu, J.; Sayyad, A.; Gibson, J. D. *J. Am. Chem. Soc.* **2006**, *128*, 15098. (c) DeVries, G. A.; Brunnbauer, M.; Hu, Y.; Jackson, A. M.; Long, B.; Neltner, B. T.; Uzun, O.; Wunsch, B. H.; Stellacci, F. *Science* **2007**, *315*, 358.
(4) Kariuki, N. N.; Han, L.; Ly, N. K.; Patterson, M. J.; Maye, M. M.; Liu, G.; Zhong, C. J. *Langmuir* **2002**, *18*, 8255.
(5) Lim, I-I. S.; Goroleski, F.; Mott, D.; Kariuki, N.; Ip, W.; Luo, J.; Zhong, C. J. *J. Phys. Chem. B* **2006**, *110*, 6673.
(6) (a) Maye, M. M.; Lim, I-I. S.; Luo, J.; Rab, Z.; Rabinovich, D.; Liu, T.; Zhong, C. J. *J. Am. Chem. Soc.* **2005**, *127*, 1519. (b) Lim, I-I. S.; Maye, M. M.; Luo, J.; Zhong, C. J. *J. Phys. Chem. B* **2005**, *109*, 2578.
(7) Hostetler, M. J.; Templeton, A. C.; Murray, R. W. *Langmuir* **1999**, *15*, 3782.
(8) Zamborini, F. P.; Hicks, J. F.; Murray, R. W. *J. Am. Chem. Soc.* **2000**, *122*, 4514.
(9) Zheng, W. X.; Maye, M. M.; Leibowitz, F. L.; Zhong, C. J. *Anal. Chem.* **2000**, *72*, 2190.
(10) Han, L.; Daniel, D. R.; Maye, M. M.; Zhong, C. J. *Anal. Chem.* **2001**, *73*, 4441.
(11) Zhong, C. J.; Maye, M. M. *Adv. Mater.* **2001**, *13*, 1507.
(12) An, D. L.; Meng, G. Y.; Zhang, Z. Y.; Zhang, L. C.; Zhang, Y. J.; Chen, Q.; Yan, H.; *Acta Chim. Sin.* **2006**, *64*, 2190.
(13) Hao, E.; Schatz, G. C. *J. Chem. Phys.* **2004**, *120*, 357.

JA071280M